Analytica Chimica Acta xxx (2014) xxx–xxx

Contents lists available at ScienceDirect

Analytica Chimica Acta

journal homepage: www.elsevier.com/locate/aca

Functionalized graphene oxide for the fabrication of paraoxon biosensors

Hangyu Zhang [a], Zhe-fei Li [b], Alexandra Snyder [c], Jian Xie [b], Lia A. Stanciu [a,c,*]

[a] Weldon School of Biomedical Engineering, Purdue University, West Lafayette, IN 47907, USA
[b] Department of Mechanical Engineering, Purdue School of Engineering and Technology, Indiana University-Purdue University Indianapolis (IUPUI), Indianapolis, IN 46202, USA
[c] School of Materials Engineering, Purdue University, West Lafayette, IN 47907, USA

HIGHLIGHTS

- We developed functionalized graphene oxide (FGO) as a platform for biosensors.
- Abundant affinity groups on FGO resulted in an excellent enzyme loading.
- The modified electrodes exhibited great short-term and long-term stability.
- The FGO biosensors showed a detection limit of 0.65 nM to paraoxon.

GRAPHICAL ABSTRACT

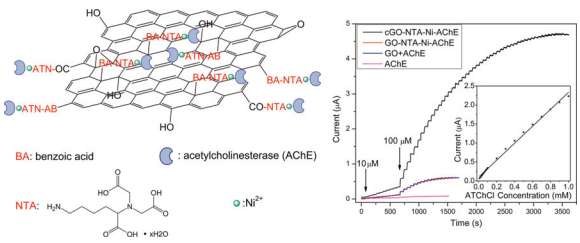

ARTICLE INFO

Article history:
Received 10 January 2014
Received in revised form 3 April 2014
Accepted 4 April 2014
Available online xxx

Keywords:
Graphene oxide
Pesticide biosensor
Functionalization
AChE
Affinity

ABSTRACT

There is an increasing need to develop biosensors for the detection of harmful pesticide residues in food and water. Here, we report on a versatile strategy to synthesize functionalized graphene oxide nanomaterials with abundant affinity groups that can capture histidine (His)-tagged acetylcholinesterase (AChE) for the fabrication of paraoxon biosensors. Initially, exfoliated graphene oxide (GO) was functionalized by a diazonium reaction to introduce abundant carboxyl groups. Then, N_α,N_α-bis (carboxymethyl)-L-lysine hydrate (NTA-NH_2) and Ni^{2+} were anchored onto the GO based materials step by step. AChE was immobilized on the functionalized graphene oxide (FGO) through the specific binding between Ni-NTA and His-tag. A low anodic oxidation potential was observed due to an enhanced electrocatalytic activity and a large surface area brought about by the use of FGO. Furthermore, a sensitivity of 2.23 μA mM^{-1} to the acetylthiocholine chloride (ATChCl) substrate was found for our composite covered electrodes. The electrodes also showed a wide linear response range from 10 μM to 1 mM (R^2 = 0.996), with an estimated detection limit of 3 μM based on an S/N = 3. The stable chelation between Ni-NTA and His-tagged AChE endowed our electrodes with great short-term and long-term stability. In addition, a linear correlation was found between paraoxon concentration and the inhibition response of the electrodes to paraoxon, with a detection limit of 6.5×10^{-10} M. This versatile strategy provides a platform to fabricate graphene oxide based nanomaterials for biosensor applications.

© 2014 Elsevier B.V. All rights reserved.

1. Introduction

Pesticide biosensors based on acetylcholinesterase (AChE) inhibition have been developed as a promising technique for the

* Corresponding author at: School of Materials Engineering, Purdue University, 701 West Stadium Avenue, West Lafayette, IN 47907, USA. Tel.: +1 765 496 3552; fax: +1 765 494 1204.
E-mail address: lstanciu@purdue.edu (L.A. Stanciu).

http://dx.doi.org/10.1016/j.aca.2014.04.014
0003-2670/© 2014 Elsevier B.V. All rights reserved.

Please cite this article in press as: H. Zhang, et al., Functionalized graphene oxide for the fabrication of paraoxon biosensors, Anal. Chim. Acta (2014), http://dx.doi.org/10.1016/j.aca.2014.04.014

analysis of organophosphate and carbamate pesticides [1–3]. These toxic compounds compose a significant class of pesticides that inhibits the normal function of AChE, which is a serine protease found at the central nervous system and functions in the synaptic transmission process, by blocking the active site on AChE [4,5]. Moreover, these pesticides that exist in food, water and soil would considerably impact safety of agricultural products and consumers' health, especially in developing countries [1]. Therefore, the development of sensitive, rapid and reliable biosensors for the detection of organophosphate and carbamate pesticides is relevant [6]. Pesticide biosensors hold the potential to complement or replace traditional analytical methods such as gas chromatography, mass spectrometry, and high-performance liquid chromatography, through the simplification or even elimination of sample preparation and the decrease of analysis time and cost [1,2]. In biosensing configurations, AChE serves as the biological element that recognizes acetylthiocholine (ATCh) and is sensitive to the inhibition by organophosporous pesticides (OP) [7,8].

Biosensors based on AChE inhibition usually employ an electrochemical detection system and involve AChE immobilization on electrode surfaces [2,3,9,10]. In an enzymatic biosensor system, the enzyme immobilization is crucial and requires the firm association between the enzyme and the substrate material, without the loss of bioactivity [11]. Immobilization methods including adsorption, entrapment and covalent coupling were applied in various nanomaterial systems for the biosensor construction [2,9,12–16]. However, adsorption and entrapment could cause enzyme leakage, leading to a poor stability of biosensors; whereas covalent coupling might result in enzyme denaturation or may not be applicable to a large range of systems. The rapid development of nanotechnology significantly impacted biosensor fabrication by providing new nanomaterials as substrate materials and novel immobilization approaches [11,17].

Graphene-based materials nowadays arouse great interest among scientists in various fields. The single-layered carbon atoms with only sp^2 bonds confer graphene outstanding properties including a considerably large specific surface area, super high mechanical strength, superior electronic properties, etc [18,19]. On the basis of their remarkable properties, graphene-based materials are found to impact the development of biomedicine [20]. Nevertheless, pure graphene tends to aggregate in aqueous solution and lacks processing capacity, rendering it to be difficult to use in biomedical systems [21]. Hence, graphene oxide (GO) and other chemically modified graphene are more widely applied in the biomedical field. With a host of oxygen functional groups on the basal plane and the sheet edge, GO displays good water solubility, good biocompatibility, and the capacity for further functionalization [21–23]. Therefore, GO was selected as the material platform for the biosensor design presented herein. Previously published work substantiate the impact of GO on the biomedical field including biosensor fabrication [13,24,25]. These studies showed that functionalization of GO can be used to achieve better biocompatibility, improved solubility in electrolyte solutions, or to obtain interaction with biomolecules or organisms at the nano/bio interfaces [26,27]. Accordingly, the development of functionalization strategies is the foundation of enzyme immobilization on graphene based nanomaterials at the nano/bio interfaces for biosensor fabrications.

The immobilization of AChE within graphene based nanomaterials introduced tremendous momentum to pesticide biosensor fabrication. A nanocomposite of chemically reduced GO and gold nanoparticles with the assistance of poly(diallyldimethylammonium chloride) (PDDA) for dispersion was synthesized for the immobilization of AChE by electrostatic interaction and ultrasensitive detection of paraoxon [13]. In another report on organophosphate pesticide detection, TiO_2 and graphene hybrids were developed for AChE immobilization by adsorption [14]. Similarly, AChE was immobilized by adsorption within the hybrid of ionic liquid and graphene [28]. The immobilization method using specific binding was also developed for AChE in a GO/gold composite system, exhibiting great potential for specific binding immobilization in terms of repeatability and stability of biosensors [29]. Graphene based nanomaterials have been used for the immobilization of various enzymes. For instance, tyrosinase-gold nanoparticles was immobilized on GO based composites for catechol detection [30]; a simple immobilization of horseradish peroxidase and lysozyme on GO was also achieved, in the absence of coupling reagents or any surface functionalization [31]. In a study where a robust immobilization approach was applied, the GO/Pt-black nanocomposites fabricated on an aqueous media platform were used to improve the sensitivity of glucose sensors [22]. In this system, glucose oxidase was crosslinked onto the GO/Pt-black composite using glutaraldehyde, which could cause enzyme activity loss and is not a versatile linker [32]. Consequently, finding novel strategies for graphene functionalization towards enhanced performance enzymatic biosensor applications is still of interest.

Here, we report on the synthesis of functionalized graphene oxide (FGO) with abundant affinity binding sites for His-tagged AChE and the application of these materials towards the fabrication of paraoxon biosensors. His-tag is widely used for recombinant protein purification, since it can be expressed at either C- or N-terminus of basically any protein with little effect on its structure and properties. This tag has affinity to Ni-NTA, which in turn can covalently react with carboxyl groups [33]. The affinity binding of His-tagged AChE with nickel(II) or cobalt(II) has been applied for AChE immobilization and the construction of pesticide biosensors in different systems, except in GO based systems [34–38]. To increase the amount of carboxyl groups especially on the basal plane of GO, we functionalized GO with 4-aminobenzoic acid (PABA) on the surface by a diazonium reaction. The PABA functionalized GO was referred to as cGO indicating the abundant carboxyl groups on it. The widely distributed Ni-NTA endowed the FGO with the ability to capture His-tagged proteins with good loading capacity. The composites were used to construct pesticide biosensors for the detection of paraoxon as a model biosensor system. The improved biosensor performance showed that the FGO could provide excellent enzyme immobilization with high enzyme loading and keep the enzyme activity for a long time.

2. Experimental

2.1. Synthesis of cGO

GO was generated and purified as described in our previous work using a modified Hummers' method [39,40]. The obtained GO was dispersed in deionized (DI) water (0.5 mg mL^{-1}, 100 mL), followed by the addition of 0.107 g PABA and 100 μL HNO_3 (68–70%). Then this mixture and 2 mL $NaNO_2$ solution (39 mM) were preheated to 65 °C. After mixing these two solutions, the mixture was shaken vigorously and kept at 65 °C for 4 h. When the reaction is completed, cGO was harvested by centrifugation at 12,000 rpm and washed with copious DI water. cGO was dispersed in DI water at a concentration of 2 mg mL^{-1} as the stock solution for further experiments.

2.2. Synthesis of cGO-NTA-Ni

The binding of NTA and Ni^{2+} onto cGO was performed using a modified method for the functionalization of carbon nanotubes [33]. N_α,N_α-Bis(carboxymethyl)-L-lysine hydrate (NTA-NH_2) was added in 2 mg mL^{-1} cGO to reach a concentration of 30 mM for

Please cite this article in press as: H. Zhang, et al., Functionalized graphene oxide for the fabrication of paraoxon biosensors, Anal. Chim. Acta (2014), http://dx.doi.org/10.1016/j.aca.2014.04.014

$NTA\text{-}NH_2$, which is much higher than the equivalent PABA concentration to guarantee sufficient $NTA\text{-}NH_2$ binding. The mixture was left overnight at room temperature for the reaction. The redundant $NTA\text{-}NH_2$ was eliminated by dialysis against DI water using 10 k MWCO dialysis tubing (Pierce). Before adding Ni^{2+}, the cGO-NTA solution was adjusted to reach a pH of 11 for a better binding ratio [33,41,42]. Then, $NiCl_2$ was introduced with a final concentration of 30 mM, an equimolar amount of original added $NTA\text{-}NH_2$, to offer adequate Ni^{2+} to chelate with NTA. After 4-h incubation of the mixture at room temperature, dialysis was applied against DI water again to remove the free Ni^{2+} together with other undesired ions. A portion of the cGO-NTA-Ni dispersed in DI water was taken out for characterization, while the rest was dialyzed against phosphate buffer saline (PBS, 0.01 M, pH 7.4, the same as below) for biosensor fabrication using 10 k MWCO dialysis tubing (Pierce). Parallel experiments were performed with GO to connect with Ni-NTA (GO-NTA-Ni) as control.

2.3. Characterization

Raman spectra were collected using a Craic Tech spectrometer with 785 nm laser excitation. For X-ray photoelectron spectroscopy (XPS), Fourier transform infrared (FTIR), and Energy-dispersive X-ray spectroscopy (EDS) tests, the solutions of our graphene-based materials were placed on silicon chips and air-dried to form thin films. XPS analysis was performed using a Kratos Ultra Axis DLD spectrometer with Al Kα monochromatic X-ray radiation (1486.69 eV). EDS data were obtained using a Philips XL-40 SEM equipped with an energy-dispersive X-ray detector. A Spectrum 100 FTIR spectrometer with a universal ATR sampling accessory (PerkinElmer) was used to record FTIR spectra. Transmission electron microscopy (TEM) images were collected with a Philips CM200 TEM operating at 200 kV.

2.4. Preparation of the pesticide biosensor

The genetically modified AChE with His-tag at the place of glycolipid anchor, which is used for in vivo linkage of the enzyme to membranes, was provided by Dr. Jean Louis Marty of University of Perpignan, France [43]. The AChE concentration before the mixture with cGO-NTA-Ni was measured based on the enzyme activity using Ellman's assay [44]. Briefly, the enzymatic activity UV/vis measurements were carried out at 412 nm ($\varepsilon = 13{,}600\ M^{-1}\ cm^{-1}$) by monitoring the appearance of a yellow compound (thionitrobenzoate) resulted by the reaction of thionitrobenzoic acid with thiocholine, the product of the enzymatic hydrolysis of acetylthiocholine substrate. 100 μL of cGO-NTA-Ni in PBS was mixed with 100 μL His-tagged AChE in PBS. After the incubation of the mixture of cGO-NTA-Ni and AChE at 4 °C overnight, excessive AChE was eliminated by dialysis against PBS using the Nanosep centrifugal device with a pore size of 200 nm (Pall). To prepare the biosensors, an aliquot of 10 μL cGO-NTA-Ni-AChE solution was placed on each glassy carbon electrode (GCE) and air-dried at room temperature. Parallel experiments were conducted with GO-NTA-Ni to form GO-NTA-Ni-AChE and evaluate the effect of diazonium reaction. The electrodes were stored in PBS at 4 °C before usage.

2.5. Electrochemical measurements

All electrochemical measurements were performed with a well-established method reported previously by our group [2,3,9]. The electrodes were tested in a cell with 3 mL PBS using a three electrode system: working electrode (modified GCE), auxiliary electrode (Pt), and reference electrode (Ag/AgCl). Acetylthiocholine chloride (ATChCl) substrate was dissolved in 0.9 wt% NaCl. Cyclic voltammetric as well as amperometric tests were carried out to characterize cGO-NTA-Ni-AChE biosensors. A calibration curve was obtained by the measurements of current responses to sequential addition of the substrate at 200 mV. As explained in Section 3, 1 mM (final concentration) was selected as the optimum substrate concentration for the subsequent amperometric tests. The operational stability testing was carried out by repetitively measuring the current response to the additions of 1 mM ATChCl. The cell was rinsed between measurements. The long-term stability was investigated by measuring the current response to 1 mM ATChCl every week. The electrodes were stored in PBS at 4 °C. Inhibition tests were conducted according to a two-step batch procedure [2,3]. Paraoxon, regarded as a model organophosphate pesticide, was dissolved in DI water. The current responses to 1 mM substrate were measured before and after the 10-min incubation of electrodes in paraoxon solutions with the concentration ranging from 10^{-10} to 10^{-5} M. At least three electrodes were used for each measurement.

3. Results and discussion

3.1. cGO

The exfoliated GO was synthesized as reported in our previous work using a modified Hummers' method [39,40,45]. The functionalization process is illustrated in Fig. 1. GO was functionalized with PABA using a diazonium reaction to introduce abundant carboxyl groups. Raman spectroscopy was used to characterize the functionalization (Fig. 2). There is no significant difference on the morphology of GO and cGO in TEM images (Fig. S1A and B). The G band located at around 1594 cm^{-1} was accounted for the sp^2 carbon signature, and the D band at about 1325 cm^{-1} was indicative of disordered aromatic structure of sp^2 carbons [46,47]. This disorder might be caused by surface defects, edges, or by the formation of sp^3 bonds, as observed in graphene functionalization. The integrated intensity ratios of D band to G band (I_D/I_G) of GO and cGO are about 0.855 and 0.972, respectively. The increase of this ratio after the diazonium reaction indicated the conversion from sp^2 to sp^3 as a result of the covalent attachment with the benzoic group onto GO surface [48].

To better investigate the functionalization of GO, XPS was applied to analyze the composition of GO and cGO. The C/O atomic ratio in GO was 2.533 based on an XPS survey scan (Fig. S2A and Table 1). By introducing benzoic acid, which has a relatively high C/O atomic ratio (3.5), this ratio increased to 3.098 for cGO, indicating a successful functionalization (Fig. S2B and Table 1). The C/O atomic ratios of GO and cGO calculated by XPS were similar with the results obtained by EDS (Table 2). Moreover, the connection of the benzoic group onto GO surface was also evidenced from the high resolution analysis of O1s spectra (Fig. 3A and B). As GO reacted with PABA, C—C bonds from the benzene ring increased along with C=O from carboxyl groups, making it difficult to evaluate the diazonium reaction in terms of C1s peaks. O1s spectra, however, were suitable for detecting the content increase of carboxyl groups by the functionalization, through which all the oxygen added were from carboxyl groups. Three major peaks decomposed from O1s spectra at 530.8 eV, 532.3 eV, and 534.2 eV were assigned to Ar—C(O)—OH, Ar—C(O)—OH, and C—OH (aromatic), in which Ar denoted aromatic carbon and the contributing oxygen atoms were underlined [49–51]. Table 3 showed these peaks and the corresponding atomic percentages. Considering that the diazonium reaction did not introduce new C—OH groups into the system, the atomic percentages of C—OH decreased from 27.8% to 2.1% implying that a considerable amount benzoic acid were connected. Consequently, abundant carboxylic acid groups were bound to the GO surface for further functionalization.

Please cite this article in press as: H. Zhang, et al., Functionalized graphene oxide for the fabrication of paraoxon biosensors, Anal. Chim. Acta (2014), http://dx.doi.org/10.1016/j.aca.2014.04.014

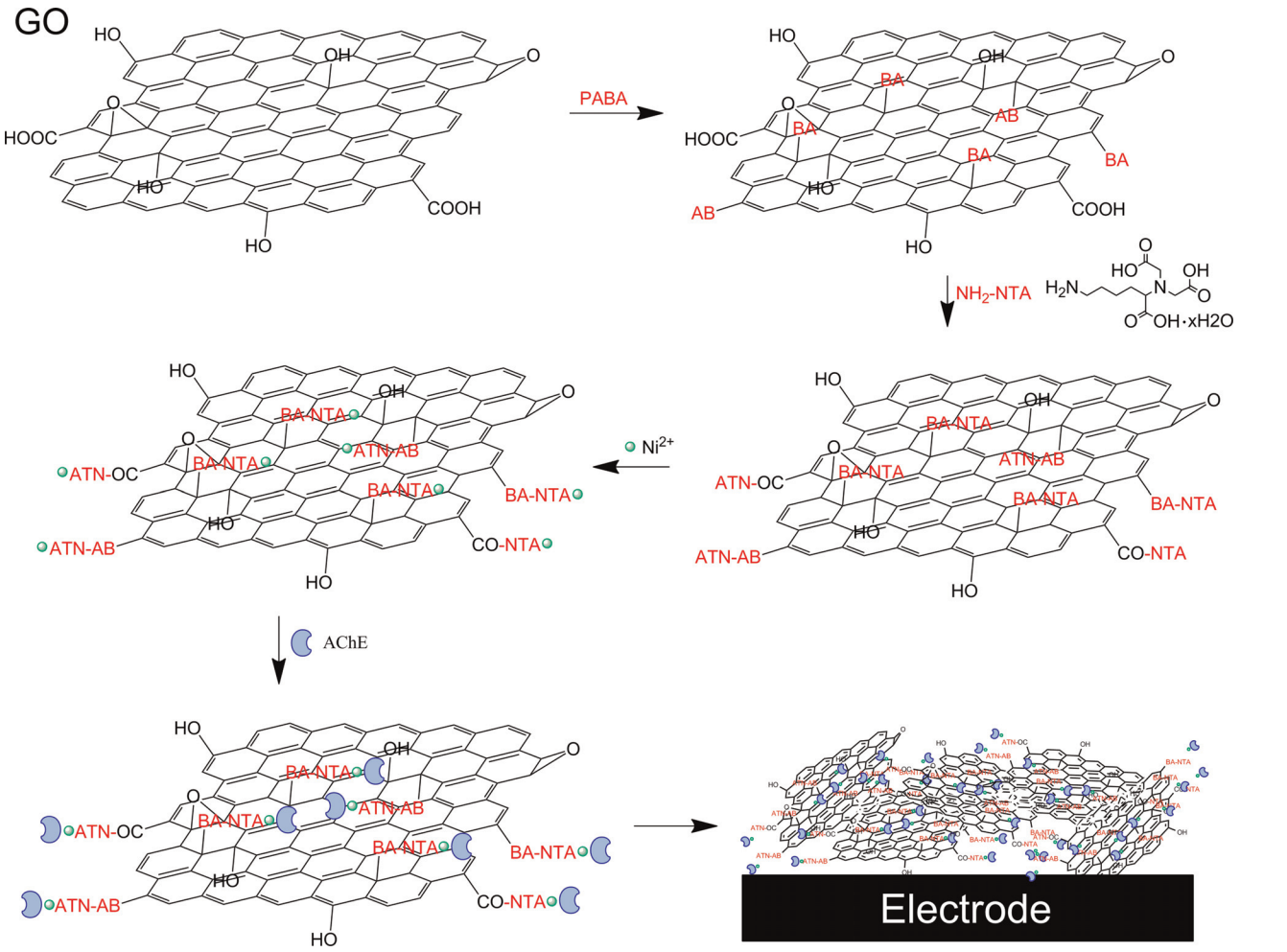

Fig. 1. Illustration of the functionalization process of GO and the resulting FGO for biosensor construction.

3.2. cGO-NTA

To realize efficient recognition and binding to specific macromolecules, the cGO was further functionalized by NTA-NH_2 and Ni^{2+} step by step. The high resolution O1s spectrum of cGO-NTA-Ni (Fig. S3) exhibited a new peak at around 531.8 eV that could be attributed to O=C—N as reported in a XPS study on tens of polymers, suggesting that a reaction of nucleophilic substitution occurred between carboxyl group and NTA-NH_2 [33,49]. Furthermore, that the C=O peak of the carboxyl group in cGO (1718 cm^{-1}) shifted to 1690 cm^{-1} (amide I band) in cGO-NTA-Ni indicated the amide bond formation as shown in the FTIR spectra (Fig. 4) [24]. Also, the peak at 1280 cm^{-1} in cGO-NTA-Ni might be ascribed to the newly formed C—N amine bond (amide III band), compared with the C—O peak at 1235 cm^{-1} from carboxyl groups in cGO [33].

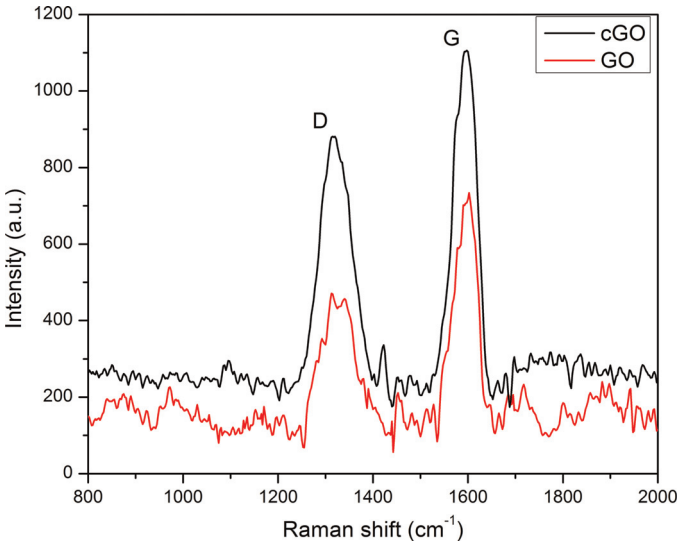

Fig. 2. Raman spectra of cGO and GO.

3.3. cGO-NTA-Ni

Given that the excess small molecules such as NTA-NH_2 and Ni^{2+} were removed by dialysis, the XPS measurements on Ni would illustrate the connection of NTA and Ni^{2+} onto the surface of cGO. A main peak at 855.4 eV accompanied by an associated wide satellite peak located at around 5.5 eV higher binding energy was identified in the high resolution spectrum of Ni 2p3/2 for the cGO-NTA-Ni

Table 1
The atomic percentage of major elements in GO and various functionalized GO measured by XPS. The unconcerned trace elements were neglected.

	GO	cGO	GO-NTA-Ni	cGO-NTA-Ni
C (%)	71.69	75.20	63.77	69.41
O (%)	28.31	24.80	34.81	27.21
Ni (%)	–	–	1.42	3.38

Please cite this article in press as: H. Zhang, et al., Functionalized graphene oxide for the fabrication of paraoxon biosensors, Anal. Chim. Acta (2014), http://dx.doi.org/10.1016/j.aca.2014.04.014

Table 2
The atomic percentage of major elements in GO and cGO measured by EDS. The trace elements that were unconcerned were neglected.

	GO	cGO
C (%)	71.54	74.95
O (%)	28.46	23.62

sample (Fig. 3C and D), which accorded with previous reports on the high resolution XPS spectrum of Ni 2p3/2 [41,42,52,53]. The appearance of the Ni 2p3/2 peak confirmed the successful functionalization of cGO by NTA-NH_2 and Ni^{2+}. The nickel atomic percentage in cGO-NTA-Ni was 3.35%, higher than the value (1.33%) in GO-NTA-Ni, calculated according to XPS measurements (Table 1). During the whole functionalization process, each nickel atom was introduced into the system along with 26 other atoms. Accordingly, the actual functionalization ratio by diazonium reaction should be much higher than 3.35%. Consequently, the cGO-NTA-Ni composite would provide adequate amount of active sites for the capture of His-tagged macromolecules.

3.4. Electrochemical characterization of the pesticide biosensors

The resulting cGO-NTA-Ni composite with immobilized AChE by nickel-histidine binding was applied to fabricate AChE-based pesticide biosensors. Considerable amount of AChE particles were bound onto the cGO surface by chelation as shown in figure S1D, whereas most of the AChE were eliminated by dialysis when cGO were simply mixed with AChE without the functionalization with Ni-NTA (Fig. S1C). The AChE-based biosensors work in an indirect electrochemical route based on the inhibition of AChE. Upon the association with AChE, ATCh is hydrolyzed into thiocholine (TCh), which is further oxidized under the applied voltage, and acetic acid if there is no inhibitor in the studied solution [3,9,12,54]:

$$\mathrm{ATCh} + \mathrm{H_2O} \overset{\mathrm{AChE}}{\rightarrow} \text{thiocholine} + \text{acetic acid} \quad (1)$$

$$2\ \text{thiocholine} \overset{\text{anodic oxidation}}{\rightarrow} \text{disulfide} + 2\mathrm{H^+} + 2\mathrm{e^-} \quad (2)$$

The electrochemical responses of cGO-NTA-Ni-AChE biosensors were on account of the anodic oxidation current of TCh (Eq. (2)). As shown in the cyclic voltammograms (CVs) of ATChCl substrate in Fig. 5, cGO-NTA-Ni-AChE covered glassy carbon electrode (GCE) exhibited a well-defined oxidation peak of TCh at around 200 mV, whereas no such peak was observed on the GO + AChE (simply mixed) covered electrode. This oxidation peak was relatively low in potential compared with some other electrode materials, such as a gold nanoparticles-graphene composite (470 mV) [13], a TiO_2-decorated graphene hybrid (700 mV) [14], and a type of reduced GO based nanocomposites (685 mV) [29]. The low anodic oxidation potential has been observed in previous reports and could be attributed to the electrocatalytic activity and the large surface area of GO based materials [2,3,54]. Moreover, on the GO-NTA-Ni-AChE covered GC electrode, a weak oxidation peak at the same potential could be seen indicating considerable improvement in AChE loading in the GO based composite upon the functionalization of GO.

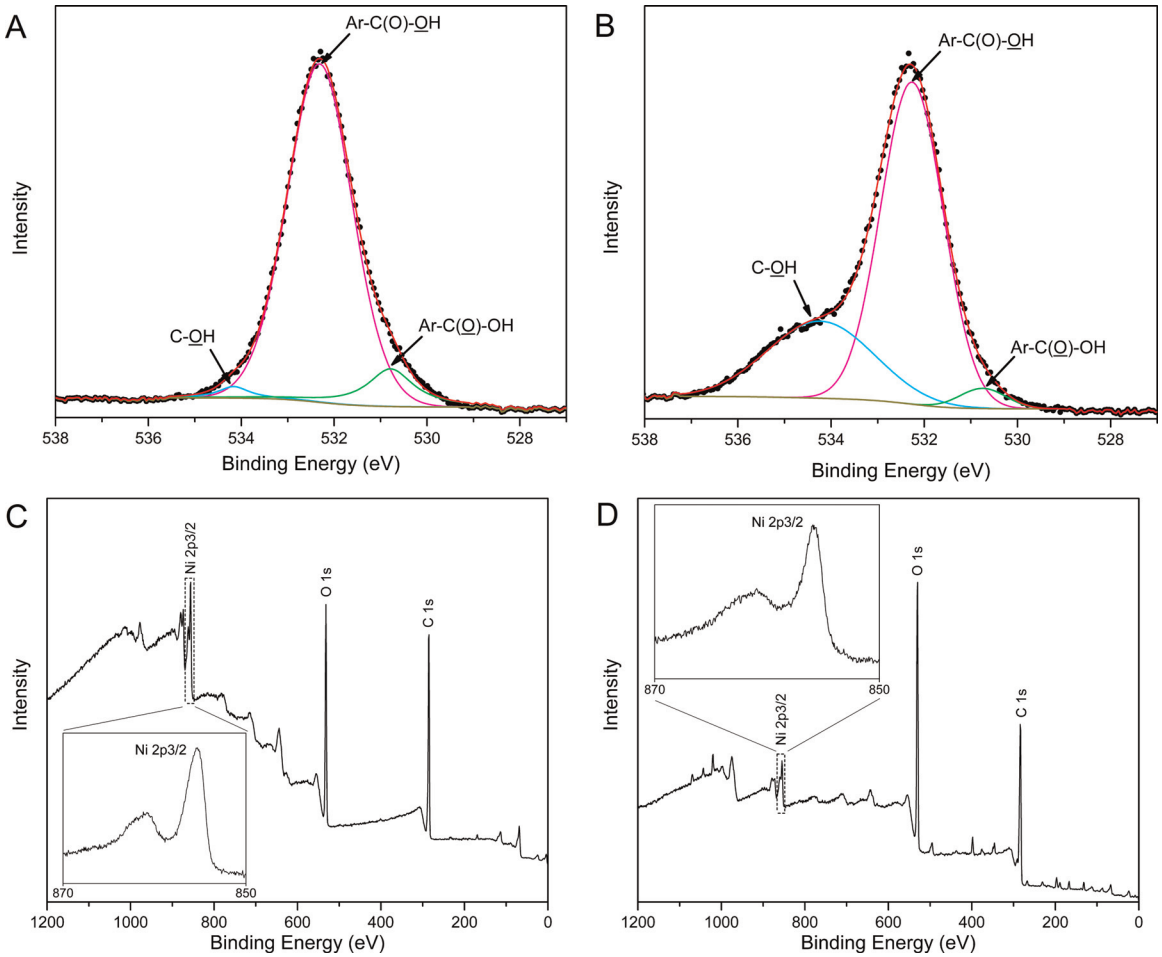

Fig. 3. XPS analysis of cGO and GO. O1s spectra of cGO (A) and GO (B). The survey spectra of cGO (C) and GO (D).

Table 3
Analysis of O1s binding energies and the atomic percentage of oxygens in different chemical states of GO and cGO.

	Ar—C(O)—OH (530.8 eV) (%)	Ar—C(O)—OH (532.3 eV) (%)	C—OH (aromatic) (534.2 eV) (%)
GO	3.2	69.0	27.8
cGO	10.2	87.7	2.1

The amperometric responses to ATChCl were investigated by successively adding the substrate (Fig. 6A). cGO-NTA-Ni-AChE biosensors exhibited a ATChCl sensitivity of ca. 2.23 μA mM^{-1}, which was more than 4 times that of biosensors modified by GO-NTA-Ni-AChE (0.53 μA mM^{-1}), and more than 27 times that of free AChE covered electrode (0.08 μA mM^{-1}). As reported previously, the incorporation of GO based composite on the electrodes could improve the biosensing performance as a result of the large surface area and the good electrochemical properties of GO materials [22,55]. The enhanced ATChCl sensing performance of cGO-NTA-Ni-AChE biosensors could be ascribed to the significantly improved AChE loading by the functionalization. Furthermore, the corresponding calibration curve (Fig. 6A inset) was used to determine the optimum concentration of ATChCl, which should be in the linear range of current response and close to the upper limit [3,54]. The electrodes coated by cGO-NTA-Ni-AChE displayed a wide linear response range spanning the concentration of ATChCl from 10 μM to 1 mM (R^2 = 0.996), showing better performance than other graphene-based material modified electrodes [13,28]. The detection limit was estimated to be 3 μM (S/N = 3) [14,28,54]. This value is lower than the detection limits reported in the literature [54,56–58]. On the basis of the calibration results, 1 mM was selected as the optimum substrate concentration for the following tests.

The stable nickel-histidine binding between cGO composite and AChE promised efficient enzyme immobilization, resulting in good short-term and long-term stabilities. Fig. 6B showed the operational stability of cGO-NTA-Ni-AChE electrodes performed by repetitively measuring the current response to the additions of

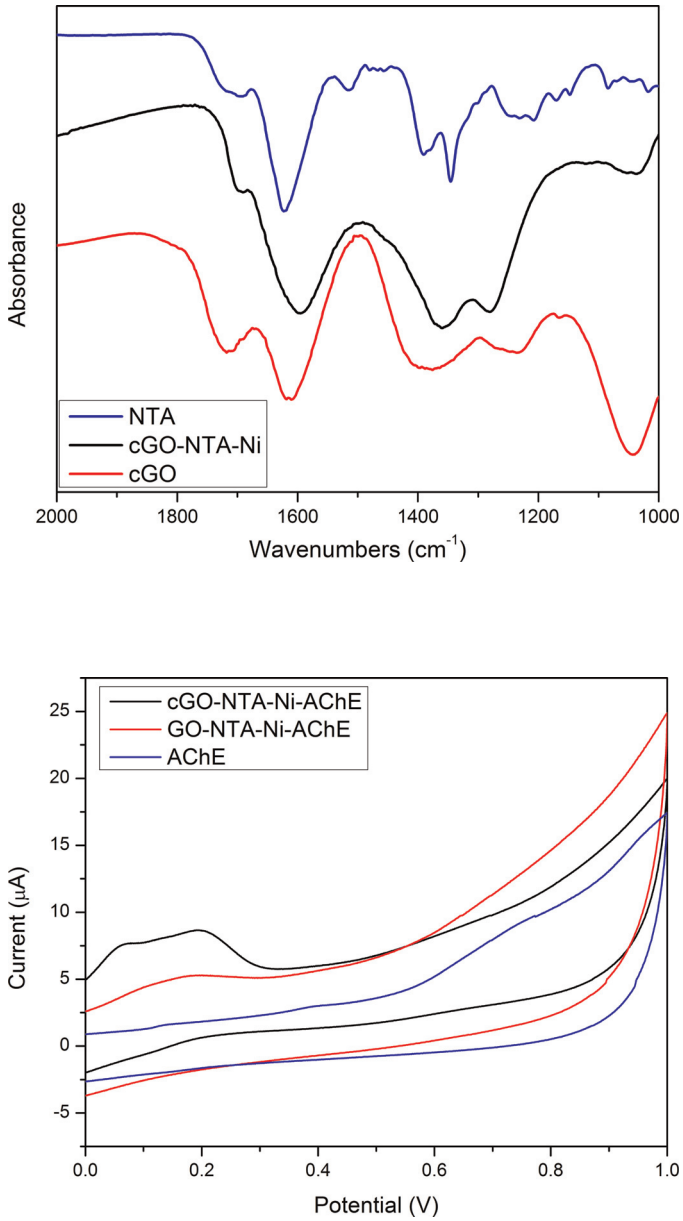

Fig. 5. Cyclic voltammetry (CV) studies of cGO-NTA-Ni-AChE, GO-NTA-Ni-AChE and AChE modified electrodes.

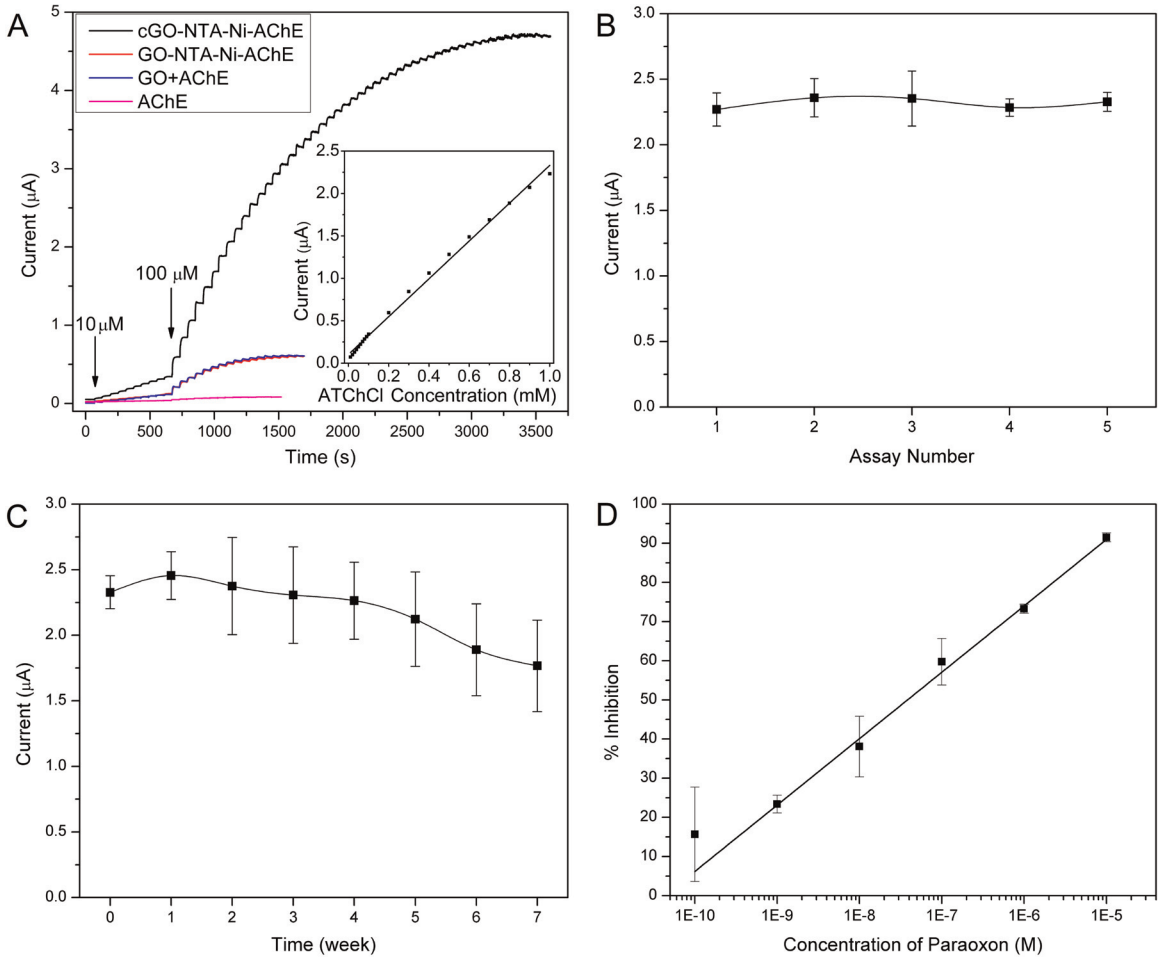

Fig. 6. (A) Representative current-time response to ATChCl of the electrodes modified by cGO-NTA-Ni-AChE, GO-NTA-Ni-AChE, GO + AChE (simply mixed), and AChE. Inset: the corresponding calibration curve of cGO-NTA-Ni-AChE modified electrodes. (B) The operational stability of cGO-NTA-Ni-AChE biosensors examined by repeated measurements. (C) The long-term stability of cGO-NTA-Ni-AChE biosensors. (D) The inhibition curve of cGO-NTA-Ni-AChE biosensors to different concentrations of paraoxon.

1 mM ATChCl. All electrodes displayed good operational stability for at least 5 assays with less than 4% response variation. Moreover, the electrodes maintained more than 97% of the enzyme activity over 4 week storage in 0.01 M PBS (pH 7.4) at 4 °C with increased current response variation (Fig. 6C). After 4 weeks, the sensitivity started to notably decrease but still maintained more than 75% of the original value after 7 weeks. The shelf life of the designed biosensors was significantly improved when compared with the biosensors based on the enzyme absorption [3,9] and entrapment [57]. Consequently, the cGO-NTA-Ni material prevented AChE from leaching and kept the enzyme activity for a long time.

In presence of paraoxon, reaction (1) is reduced or even totally inhibited. The oxidation current is found to be correlated to the pesticide concentration if certain exposure time is applied. The current response of cGO-NTA-Ni-AChE modified electrodes was measured in the absence of paraoxon and then measured again after 10 min incubation of the electrodes in paraoxon solution with different concentration. The paraoxon concentration was quantitatively related to the decrease of current response by the inhibition, which was calculated based on the following reaction [3,9]:

$$\text{Inhibition}(\%) = \frac{\text{initial current} - \text{final current}}{\text{initial current}} \times 100 \quad (3)$$

The relation of paraoxon concentration and the inhibition response was plotted in Fig. 6D. As shown, the reduction current as a result of AChE inhibition was basically linearly correlated to the log of paraoxon concentration in the measurement range with a linearity regression equation of $y = 16.96\log_{10}x + 175.78$ ($R^2 = 0.998$) , in which y is % inhibition and x is the paraoxon concentration. A paraoxon detection limit of 6.5×10^{-10} M was calculated for 20% inhibition. The detection limit was lower than other biosensors reported previously (Table S1).Although good biosensor performance in terms of short- and long-term stability and sensitivity to paraoxon was achieved with the reported configuration, the inherent weakness of enzyme inhibition-based biosensors, i.e., the lack of selectivity, might limit their application. Specifically, in addition to organophosphate and carbamate pesticides, which are the target analytes, many other chemicals, such as metal cations, organic compounds, and inorganic species could inhibit the activity of AChE, thereby leading to false positive results [59,60]. Consequently, inhibition-based pesticide biosensors could probably be best used for general sample screening before significant advances in the selectivity are made. Here, we focused our efforts on the development of a new strategy to fabricate FGO with abundant affinity groups towards His-tagged AChE. Accordingly, the selectivity problem of enzyme inhibition-based biosensors was not addressed by the scope of this report. Finally, a benefit of the FGO with abundant affinity groups developed in current research is that it can theoretically bind to any His-tagged proteins, and hence provide a potential platform for versatile biosensor design.

Please cite this article in press as: H. Zhang, et al., Functionalized graphene oxide for the fabrication of paraoxon biosensors, Anal. Chim. Acta (2014), http://dx.doi.org/10.1016/j.aca.2014.04.014

4. Conclusion

In this work, we developed FGO with strong affinity to His-tagged AChE for the fabrication of paraoxon biosensors. The AChE was selected as the model enzyme to evaluate the functionalization and the potential of FGO as versatile enzyme immobilization nanomaterials for the biosensor deign. With diversified characterization techniques, adequate amount of Ni-NTA was found to connect on the GO surface, which led to good enzyme loading, improved electrocatalytic activities and sensitivity. Moreover, excellent short-term and long-term stability were also observed due to the stable binding between Ni-NTA and His-tagged AChE. The inhibition response was linearly correlated to the paraoxon concentrations with a detection limit of 6.5×10^{-10} M. The designed FGO composite can be adapted to versatile biosensor fabrication.

Acknowledgments

The authors are grateful for the financial support provided by the National Science Foundation DMR #0804464. The XPS data were collected at the Surface Analysis Facility of the Birck Nanotechnology Center, Purdue University.

Appendix A. Supplementary data

Supplementary data associated with this article can be found, in the online version, at http://dx.doi.org/10.1016/j.aca.2013.12.001.

References

[1] C.S. Pundir, N. Chauhan, Acetylcholinesterase inhibition-based biosensors for pesticide determination: a review, Analytical Biochemistry 429 (2012) 19–31.
[2] R. Sinha, M. Ganesana, S. Andreescu, L. Stanciu, AChE biosensor based on zinc oxide sol–gel for the detection of pesticides, Analytica Chimica Acta 661 (2010) 195–199.
[3] Y.-H. Won, H.S. Jang, S.M. Kim, E. Stach, M. Ganesana, S. Andreescu, L.A. Stanciu, Biomagnetic Glasses:, Preparation, characterization, and biosensor applications, Langmuir 26 (2009) 4320–4326.
[4] D.M. Quinn, Acetylcholinesterase: enzyme structure, reaction dynamics, and virtual transition states, Chemical Reviews 87 (1987) 955–979.
[5] P. Taylor, Z. Radic, The cholinesterases: from genes to proteins, Annual Review of Pharmacology and Toxicology 34 (1994) 281–320.
[6] J. Zhang, A. Luo, P. Liu, S. Wei, G. Wang, S. Wei, Detection of organophosphorus pesticides using potentiometric enzymatic membrane biosensor based on methylcellulose immobilization, Analytical Sciences 25 (2009) 511–515.
[7] M. Wang, X. Gu, G. Zhang, D. Zhang, D. Zhu, Continuous colorimetric assay for acetylcholinesterase and inhibitor screening with gold nanoparticles, Langmuir 25 (2009) 2504–2507.
[8] A.A. Weinbroum, Pathophysiological and clinical aspects of combat anticholinesterase poisoning, British Medical Bulletin 72 (2005) 119–133.
[9] A. Snyder, Z. Bo, Q. Sun, C. Martinez, L. Stanciu, Electrochemical biosensors fabricated with polyelectrolyte microspheres, Journal of the Electrochemical Society 159 (2012) B783–B788.
[10] Y.-H. Won, H.S. Jang, D.-W. Chung, L.A. Stanciu, Multifunctional calcium carbonate microparticles: synthesis and biological applications, Journal of Materials Chemistry 20 (2010) 7728–7733.
[11] L. Stanciu, Y.-H. Won, M. Ganesana, S. Andreescu, Magnetic particle-based hybrid platforms for bioanalytical sensors, Sensors 9 (2009) 2976–2999.
[12] J. Dong, X. Fan, F. Qiao, S. Ai, H. Xin, A novel protocol for ultra-trace detection of pesticides: combined electrochemical reduction of Ellman's reagent with acetylcholinesterase inhibition, Analytica Chimica Acta 761 (2013) 78–83.
[13] Y. Wang, S. Zhang, D. Du, Y. Shao, Z. Li, J. Wang, M.H. Engelhard, J. Li, Y. Lin, Self assembly of acetylcholinesterase on a gold nanoparticles-graphene nanosheet hybrid for organophosphate pesticide detection using polyelectrolyte as a linker, Journal of Materials Chemistry 21 (2011) 5319–5325.
[14] K. Wang, H.-N. Li, J. Wu, C. Ju, J.-J. Yan, Q. Liu, B. Qiu, TiO_2-decorated graphene nanohybrids for fabricating an amperometric acetylcholinesterase biosensor, Analyst 136 (2011) 3349–3354.
[15] J. Shi, T.-G. Cha, J.C. Claussen, A.R. Diggs, J.H. Choi, D.M. Porterfield, Microbiosensors based on DNA modified single-walled carbon nanotube and Pt-black nanocomposites, Analyst 136 (2011) 4916–4924.
[16] Y. Li, L. Zhang, M. Li, Z. Pan, D. Li, A disposable biosensor based on immobilization of laccase with silica spheres on the MWCNTs-doped screen-printed electrode, Chemistry Central Journal 6 (2012) 1–8.
[17] F. Patolsky, G. Zheng, C.M. Lieber, Nanowire-based biosensors, Analytical Chemistry 78 (2006) 4260–4269.
[18] K.R. Ratinac, W.R. Yang, J.J. Gooding, P. Thordarson, F. Braet, Graphene and related materials in electrochemical sensing, Electroanalysis 23 (2011) 803–826.
[19] M. Pumera, A. Ambrosi, A. Bonanni, E.L.K. Chng, H.L. Poh, Graphene for electrochemical sensing and biosensing, Trac-Trends in Analytical Chemistry 29 (2010) 954–965.
[20] H. Zhang, G. Gruner, Y. Zhao, Recent advancements of graphene in biomedicine, Journal of Materials Chemistry B 1 (2013) 2542–2567.
[21] T. Kuila, S. Bose, A.K. Mishra, P. Khanra, N.H. Kim, J.H. Lee, Chemical functionalization of graphene and its applications, Progress in Materials Science 57 (2012) 1061–1105.
[22] J. Shi, H. Zhang, A. Snyder, M. -x. Wang, J. Xie, D. Marshall Porterfield, L.A. Stanciu, An aqueous media based approach for the preparation of a biosensor platform composed of graphene oxide and Pt-black, Biosensors and Bioelectronics 38 (2012) 314–320.
[23] J. Kim, L.J. Cote, J. Huang, Two dimensional soft material: new faces of graphene oxide, Accounts of Chemical Research 45 (2012) 1356–1364.
[24] X. Sun, Z. Liu, K. Welsher, J. Robinson, A. Goodwin, S. Zaric, H. Dai, Nano-graphene oxide for cellular imaging and drug delivery, Nano Research 1 (2008) 203–212.
[25] Z. Liu, J.T. Robinson, X. Sun, H. Dai, PEGylated nanographene oxide for delivery of water-insoluble cancer drugs, Journal of the American Chemical Society 130 (2008) 10876–10877.
[26] Y. Wang, Z.H. Li, J. Wang, J.H. Li, Y.H. Lin, Graphene and graphene oxide: biofunctionalization and applications in biotechnology, Trends in Biotechnology 29 (2011) 205–212.
[27] B.J. Hong, O.C. Compton, Z. An, I. Eryazici, S.T. Nguyen, Successful stabilization of graphene oxide in electrolyte solutions: enhancement of biofunctionalization and cellular uptake, ACS Nano 6 (2011) 63–73.
[28] Y. Li, G. Han, Ionic liquid-functionalized graphene for fabricating an amperometric acetylcholinesterase biosensor, Analyst 137 (2012) 3160–3165.
[29] T. Liu, H. Su, X. Qu, P. Ju, L. Cui, S. Ai, Acetylcholinesterase biosensor based on 3-carboxyphenylboronic acid/reduced graphene oxide–gold nanocomposites modified electrode for amperometric detection of organophosphorus and carbamate pesticides, Sensors and Actuators B: Chemical 160 (2011) 1255–1261.
[30] W. Song, D.-W. Li, Y.-T. Li, Y. Li, Y.-T. Long, Disposable biosensor based on graphene oxide conjugated with tyrosinase assembled gold nanoparticles, Biosensors and Bioelectronics 26 (2011) 3181–3186.
[31] J. Zhang, F. Zhang, H. Yang, X. Huang, H. Liu, J. Zhang, S. Guo, Graphene oxide as a matrix for enzyme immobilization, Langmuir 26 (2010) 6083–6085.
[32] J. House, E. Anderson, K. Ward, Immobilization techniques to avoid enzyme loss from oxidase-based biosensors: a one-year study, Journal of diabetes science and technology 1 (2007) 18–27.
[33] R.A. Graff, T.M. Swanson, M.S. Strano, Synthesis of nickel–nitrilotriacetic acid coupled single-walled carbon nanotubes for directed self-assembly with polyhistidine-tagged proteins, Chemistry of Materials 20 (2008) 1824–1829.
[34] S. Andreescu, L. Barthelmebs, J.-L. Marty, Immobilization of acetylcholinesterase on screen-printed electrodes: comparative study between three immobilization methods and applications to the detection of organophosphorus insecticides, Analytica Chimica Acta 464 (2002) 171–180.
[35] M. Ganesana, G. Istarnboulie, J.-L. Marty, T. Noguer, S. Andreescu, Site-specific immobilization of a (His)6-tagged acetylcholinesterase on nickel nanoparticles for highly sensitive toxicity biosensors, Biosensors and Bioelectronics 30 (2011) 43–48.
[36] R.K. Mishra, R.B. Dominguez, S. Bhand, R. Muñoz, J.-L. Marty, A novel automated flow-based biosensor for the determination of organophosphate pesticides in milk, Biosensors and Bioelectronics 32 (2012) 56–61.
[37] G. Istamboulie, M. Cortina-Puig, J.-L. Marty, T. Noguer, The use of artificial neural networks for the selective detection of two organophosphate insecticides: chlorpyrifos and chlorfenvinfos, Talanta 79 (2009) 507–511.
[38] G. Istamboulie, S. Andreescu, J.-L. Marty, T. Noguer, Highly sensitive detection of organophosphorus insecticides using magnetic microbeads and genetically engineered acetylcholinesterase, Biosensors and Bioelectronics 23 (2007) 506–512.
[39] Z.-F. Li, H. Zhang, Q. Liu, L. Sun, L. Stanciu, J. Xie, Fabrication of high-surface-area graphene/polyaniline nanocomposites and their application in supercapacitors, ACS Applied Materials & Interfaces 5 (2013) 2685–2691.
[40] M.-x. Wang, Q. Liu, H.-f. Sun, E.A. Stach, H. Zhang, L. Stanciu, J. Xie, Preparation of high-surface-area carbon nanoparticle/graphene composites, Carbon 50 (2012) 3845–3853.
[41] J.K. Lee, Y.-G. Kim, Y.S. Chi, W.S. Yun, I.S. Choi, Grafting nitrilotriacetic groups onto carboxylic acid-terminated self-assembled monolayers on gold surfaces for immobilization of Histidine-tagged proteins, The Journal of Physical Chemistry B 108 (2004) 7665–7673.
[42] G.B. Sigal, C. Bamdad, A. Barberis, J. Strominger, G.M. Whitesides, A self-assembled monolayer for the binding and study of Histidine-tagged proteins by surface plasmon resonance, Analytical Chemistry 68 (1996) 490–497.
[43] S. Andreescu, V. Magearu, A. Lougarre, D. Fournier, J.L. Marty, Immobilization of enzymes on screen-printed sensors via an histidine tail. Application to the detection of pesticides using modified cholinesterase, Analytical Letters 34 (2001) 529–540.

Please cite this article in press as: H. Zhang, et al., Functionalized graphene oxide for the fabrication of paraoxon biosensors, Anal. Chim. Acta (2014), http://dx.doi.org/10.1016/j.aca.2014.04.014

[44] G.L. Ellman, K.D. Courtney, V. Andres Jr, R.M. Featherstone, A new and rapid colorimetric determination of acetylcholinesterase activity, Biochemical Pharmacology 7 (1961) 88–95.
[45] W.S. Hummers, R.E. Offeman, Preparation of graphitic oxide, Journal of the American Chemical Society 80 (1958) 1339.
[46] G. Zeb, P. Gaskell, X.T. Le, X. Xiao, T. Szkopek, M. Cerruti, Decoration of graphitic surfaces with sn nanoparticles through surface functionalization using diazonium chemistry, Langmuir 28 (2012) 13042–13050.
[47] A.C. Ferrari, J.C. Meyer, V. Scardaci, C. Casiraghi, M. Lazzeri, F. Mauri, S. Piscanec, D. Jiang, K.S. Novoselov, S. Roth, A.K. Geim, Raman spectrum of graphene and graphene layers, Physical Review Letters 97 (2006) 187401.
[48] J.R. Lomeda, C.D. Doyle, D.V. Kosynkin, W.-F. Hwang, J.M. Tour, Diazonium functionalization of surfactant-wrapped chemically converted graphene sheets, Journal of the American Chemical Society 130 (2008) 16201–16206.
[49] D. Briggs, G. Beamson, XPS studies of the oxygen 1s and 2s levels in a wide range of functional polymers, Analytical Chemistry 65 (1993) 1517–1523.
[50] S.H. Shim, K.T. Kim, J.U. Lee, W.H. Jo, Facile method to functionalize graphene oxide and its application to poly(ethylene terephthalate)/graphene composite, ACS Applied Materials & Interfaces 4 (2012) 4184–4191.
[51] A. Ganguly, S. Sharma, P. Papakonstantinou, J. Hamilton, Probing the thermal deoxygenation of graphene oxide using high-resolution in situ X-ray-based spectroscopies, The Journal of Physical Chemistry C 115 (2011) 17009–17019.
[52] O. Du Roure, C. Debiemme-Chouvy, J. Malthête, P. Silberzan, Functionalizing surfaces with nickel ions for the grafting of proteins, Langmuir 19 (2003) 4138–4143.
[53] H.W. Nesbitt, D. Legrand, G.M. Bancroft, Interpretation of Ni2p XPS spectra of Ni conductors and Ni insulators, Phys Chem Min 27 (2000) 357–366.
[54] G. Liu, Y. Lin, Biosensor based on self-assembling acetylcholinesterase on carbon nanotubes for flow injection/amperometric detection of organophosphate pesticides and nerve agents, Analytical Chemistry 78 (2006) 835–843.
[55] T. Kuila, S. Bose, P. Khanra, A.K. Mishra, N.H. Kim, J.H. Lee, Recent advances in graphene-based biosensors, Biosensors and Bioelectronics 26 (2011) 4637–4648.
[56] F.E. Kanik, M. Kolb, S. Timur, M. Bahadir, L. Toppare, An amperometric acetylcholine biosensor based on a conducting polymer, International Journal of Biological Macromolecules 59 (2013) 111–118.
[57] M. Yang, Y. Yang, Y. Yang, G. Shen, R. Yu, Microbiosensor for acetylcholine and choline based on electropolymerization/sol–gel derived composite membrane, Analytica Chimica Acta 530 (2005) 205–211.
[58] A.N. Ivanov, R.R. Younusov, G.A. Evtugyn, F. Arduini, D. Moscone, G. Palleschi, Acetylcholinesterase biosensor based on single-walled carbon nanotubes – Co phtalocyanine for organophosphorus pesticides detection, Talanta 85 (2011) 216–221.
[59] J.S. Van Dyk, B. Pletschke, Review on the use of enzymes for the detection of organochlorine, organophosphate and carbamate pesticides in the environment, Chemosphere 82 (2011) 291–307.
[60] M.D. Luque de Castro, M.C. Herrera, Enzyme inhibition-based biosensors and biosensing systems: questionable analytical devices, Biosensors and Bioelectronics 18 (2003) 279–294.

Please cite this article in press as: H. Zhang, et al., Functionalized graphene oxide for the fabrication of paraoxon biosensors, Anal. Chim. Acta (2014), http://dx.doi.org/10.1016/j.aca.2014.04.014